Low-loss grating-coupled optical interfaces for large-volume fabrication with deep-ultraviolet optical lithography

Daniel Benedikovic, Carlos Alberto Alonso-Ramos, Sylvain Guerber, Diego Pérez-Galacho, Vladyslav Vakarin, Guillaume Marcaud, Xavier Le Roux, Eric Cassan, Delphine Marris-Morini, Pavel Cheben, et al.

HAL Id: hal-01800594
https://hal.science/hal-01800594

Submitted on 18 Sep 2018

Low-loss grating-coupled optical interfaces for large-volume fabrication with deep-ultraviolet optical lithography

Daniel Benedikovic[a], Carlos Alberto Alonso-Ramos[a], Sylvain Guerber[a,b], Diego Pérez-Galacho[a],
Vladyslav Vakarin[a], Guillaume Marcaud[a], Xavier Le Roux[a], Eric Cassan[a], Delphine Marris-Morini[a],
Pavel Cheben[c], Frederic Boeuf[b], Charles Baudot[b], and Laurent Vivien[a]

[a]Centre de Nanoscience et de Nanotechnology, CNRS, Univ. Paris-Sud, Université Paris-Saclay,
C2N-Orsay, 91405 Orsay Cedex, France;
[b]TR&D-STMicroelectronics SAS-850 rue Jean Monnet-38920 Crolles, France;
[c]National Research Council Canada, 1200 Montreal Road, Ottawa, Ontario, K1A0R6, Canada

ABSTRACT

Optical input/output interfaces between silicon-on-insulator (SOI) waveguides and optical fibers, allowing robust, cost-effective and low-loss coupling of light, are fundamental functional elements in the library of silicon photonic devices. Surface grating couplers are particularly desirable as they allow wafer-scale device testing, yield improved alignment tolerances, and are compatible with state-of-the-art integration and packaging technologies. While several factors jointly contribute to the coupler performance, the grating directionality is a critical parameter for high-efficiency fiber-chip coupling. To address this issue, conventional coupler designs typically call upon comparatively complex architectures to improve light coupling efficiency. Increasing the intrinsic directionality of the grating by exploiting the blazing effects is another promising solution. In this paper, we report on our recent advances in development of low-loss grating couplers that afford excellent directionality, close to the theoretical limit of 100%. In particular, we demonstrate, by theory and experiments, several implementations of blazed grating couplers with layout features that are compatible with deep-ultraviolet (deep-UV) optical lithography. Devices can be advantageously implemented on various photonic platforms, including industry-specific and the offerings of publicly accessible foundries. The first experimental realizations of uniform deep-UV-compatible couplers yield losses of -2.7 dB at 1.55-µm and a 3-dB bandwidth of 62 nm. A subwavelength-index-engineered impedance matching transition is used to reduce back-reflections down to -20 dB.

Keywords: Silicon photonics, single-mode optical fiber, surface grating couplers, sub-wavelength grating metamaterials, deep-ultraviolet optical lithography, complementary metal-oxide-semiconductor technology

1. INTRODUCTION

Silicon-on-insulator (SOI) has become a compelling material platform for silicon photonics in order to realize nano-scale integrated devices. This is partly due to the compatibility with the established manufacturing tools, techniques, and testing processes developed by the industries of micro-electronics and fiber optic telecommunications. Furthermore, the fabrication services of silicon nanophotonic foundries has become widely accessible, thereby opening a new route for the fabless development of complex photonic integrated circuits that contain hundreds or even thousands of different components on a single silicon (Si) chip[1-5]. However, the sub-micrometric cross-sectional dimensions of SOI waveguides imposes a fundamental challenge for the efficient coupling of light to or from external optical ports[5-10].

Optical interfacing between fibers and SOI nanophotonic platforms that ensure improved fabrication tolerance, reduced cost, and low-loss coupling are greatly recognized to be crucial on-chip functions in integrated photonics. In this context, surface grating couplers play elementary, yet substantial role for a widespread deployment. Grating-coupled optical interfaces allow a flexible positioning on the Si chip, thereby enabling wafer-scale device characterization, preferred for mass-volume scenarios[5-8]. In addition, the surface coupling structures afford enhanced alignment tolerances in comparison to the edge couplers[9, 10] as well as are compatible with integration and packaging technologies[4-8].

Surface grating couplers, with an out-of-plane coupling layout, are particularly unique components in the library of silicon photonic devices. They inherently desire a high vertical index contrast to provide an outstanding fiber-chip coupling. However, overall coupling efficiency is restricted by several factors. This mainly encompasses the back-reflections at the waveguide-to-grating junction, the mode size disparity between the Gaussian-like optical fiber mode and the exponential decaying profile of the diffracted grating beam, as well as the parasitic optical power radiated into

the bottom Si substrate. The first two issues may simultaneously be addressed by grating coupler apodization[11-18]. This includes approaches such as an etch depth variation[11], a duty cycle optimization[12, 13], or a sub-wavelength grating (SWG) refractive index engineering[14-18]. However, the limited diffraction efficiency of the grating towards the optical fiber, also known as a grating directionality, is a significant challenge.

The improvement of the grating diffraction performance may be achieved by exploiting the effect of thin-film interference via optimization of the radiation angle[16-18]. Additional techniques to enhance the directionality include supplementary high- or low-index overlayers[19-22], backside wafer metallization[23-25], distributed single or multi-layer Bragg reflectors[26, 27], multi-level grating architectures[28-30], or customized etch depths[11, 31, 32]. However, afore-described approaches typically result in comparatively complex structures, with the expense of specific fabrication steps and extra processing costs. As an alternative, it has been shown, both theoretically and experimentally, that the blazing effect may advantageously be exploited to achieve remarkably high grating directionalities[33-39]. Nevertheless, in many proof-of-concept demonstrations[33-38], high-efficiency blazed grating couplers were fabricated using a time-consuming and rather expensive electron beam (e-beam) lithography. Albeit proven useful, e-beam lithography systems are not suitable, especially due to lack of compatibility with large-volume industry-oriented applications. On the other hand, recent research works also suggest that the migration from 220-nm-thick SOI platforms towards their thicker counterparts[4-6, 8], especially 300-nm-thick Si films, may be advantageous in terms of improving the performance of other passive and active photonic devices[5, 8, 40].

In this work, we report our results on the design, fabrication, and experiments of a high-directionality fiber-chip grating coupler, being seamlessly fabricated by using 193-nm deep-ultraviolet (deep-UV) photolithography. The grating coupler is implemented on a 300-nm-thick Si film in a 300 mm SOI wafer, relying on the combined deep (300 nm) and partial (150 nm) etching steps. More specifically, the proposed blazed grating coupler design, favoring a L-shaped device geometry, yields an eminently high directionality, exceeding 98%, with a reduced fabrication complexity compared to the previously demonstrated blazed coupling structures[33-36]. Experimentally, a total fiber-chip coupling loss up to -2.7 dB is demonstrated, with a 3-dB coupling bandwidth of 62 nm. Furthermore, the inclusion of a short SWG-index-engineered transition affords a noticeable reduction of the measured grating reflectivity, down to -20 dB.

This paper is organized as follows. After the introductory *Section 1*, the *Section 2* describes the design of L-shaped high-directionality grating couplers. In *Section 3*, we describe the fabrication, characterization, and achieved experimental results. *Section 4* provides a theoretical outlook towards the development of sub-decibel L-shaped coupling structures. Finally, conclusions are drawn in *Section 5*.

2. DEVICE DESIGN

Schematic views of the proposed L-shaped fiber-chip grating coupler with a SWG transition is shown in Figure 1.
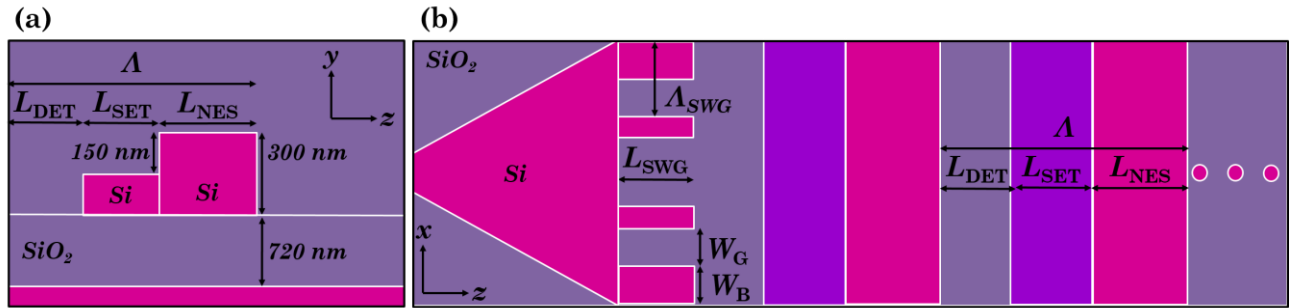

Figure 1. Schematics of a L-shaped fiber-chip grating coupler: (a) side (y-z plane) view and (b) top (x-z plane) view.

The grating diffraction period (Λ) is composed of deep- and shallow-etch trenches, with lengths denoted as L_{DET} and L_{SET}, respectively, and a non-etched Si strip of a length L_{NES}. Here, the deep- and the partial-etched levels are set to be 300 nm and 150 nm, respectively, for the definition of the grating coupler pattern. The device is optimized for a coupling of light with a transverse electrical (TE) polarization state, operating in a conventional optical communication band (C-band), near a central wavelength of 1.55 μm. The designs of grating couplers were performed by using a two-dimensional (2-D) Fourier-based tool[41] and a three-dimensional (3-D) Finite Difference Time Domain (FDTD) simulator, from Lumerical[42].

The *L*-shaped grating arrangement advantageously exploits the blazing effect for an extraordinary ultra-high diffraction performance, in which the optical power radiated towards the superstrate (upper cladding) is maximized, while the parasitic radiation of optical power into the bottom Si substrate is minimized. In this work, we define the grating directionality as the ratio between the power diffracted towards the upper cladding, where the optical fiber is situated, and the total out-coupled optical power (the sum of a power diffracted towards the superstrate and substrate).

At a first design stage, we optimized the grating coupler dimensions without a SWG grating transition. In Figure 2a - 2c are shown 2-D calculations of the grating coupler directionality as a function of the length of the shallow-etch (L_{SET}) and the non-etched (L_{NES}) grating segments. Here, different lengths of the deep-etched grating trenches (L_{DET}) were considered ($L_{DET} = 50$ nm; $L_{DET} = 100$ nm; and $L_{DET} = 150$ nm). From this analysis, it became apparent that a broad span of grating geometries are viable to provide a high diffraction performance, typically higher than 90%, which in turn, also suggests relatively large tolerance in respect to the presence of fabrication errors. The following dimensions of the nominal grating coupler were chosen: $L_{DET} = 120$ nm; $L_{SET} = 290$ nm; and $L_{NES} = 310$ nm[39]. This particular geometry affords a directionality of 98%. Furthermore, Figure 2d shows a grating directionality as a function of the depth variation in partially etched grating trenches, also proving an excellent tolerance to fabrication imperfections. The spectral performance of the grating directionality is shown in Figure 2e.
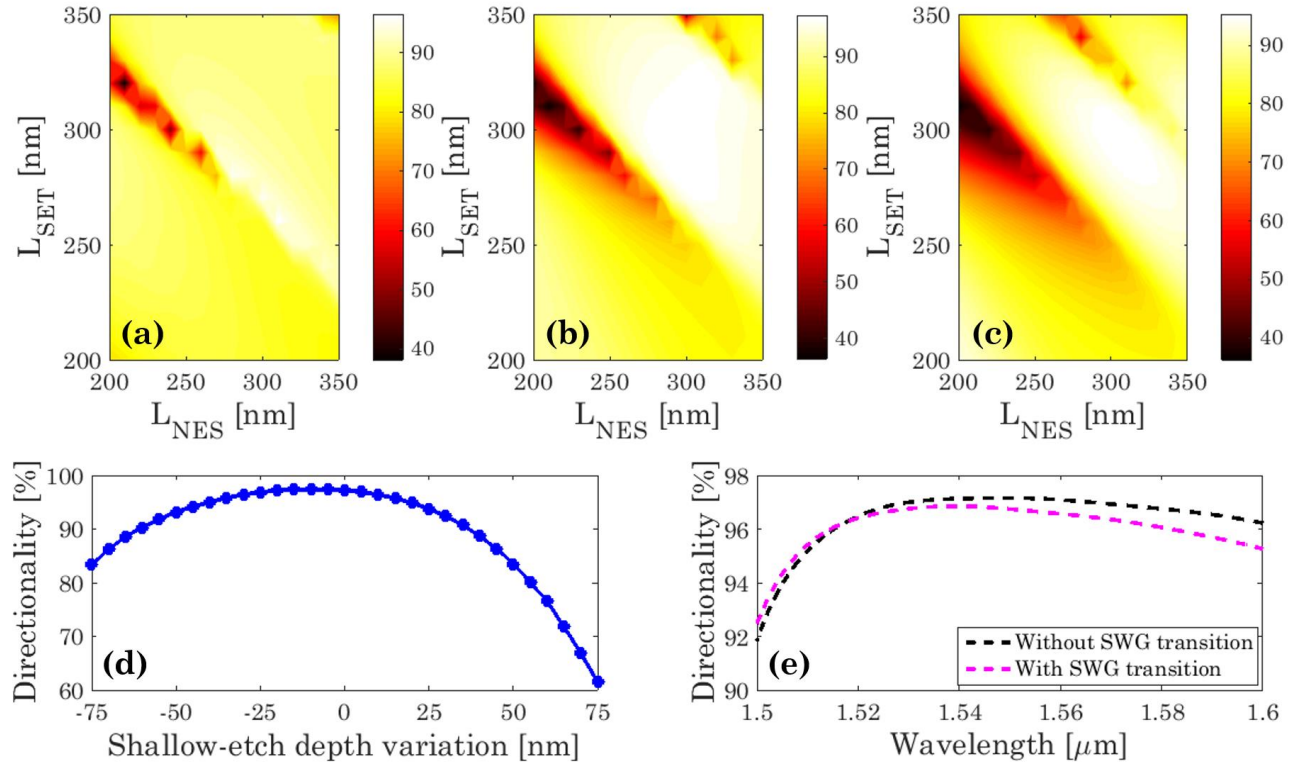

Figure 2. 2-D contour maps of the directionality as a function of shallow- and non-etched grating segments, for different lengths of a deep-etched trenches: (a) $L_{DET} = 50$ nm; (b) $L_{DET} = 100$ nm; and (c) $L_{DET} = 150$ nm. (d) Directionality as a function of the partial etch depth in grating trenches. (e) Spectral evolution of the directionality for nominal grating coupler designs, with and without the SWG transition stage, as predicted by 3-D FDTD calculations.

At a next phase of device design, we implemented a short SWG metamaterial transition stage between the injection waveguide and the grating in order to control the back-reflections. This metamaterial-based transition has been realized by exploiting the concept of SWG nano-structuration. This technologically profound concept was demonstrated for the first time in Refs.[43-45], and most recently, extensively utilized in a variety of photonic devices[46], including components for wideband[47-49] and narrowband[50-52] spectral operation, sensing structures[53-55], or waveguides for extended mid-infrared (mid-IR) wavelengths[56, 57], to name a few outstanding implementations.

More specifically, the SWG anti-reflection transition was implemented along the transversal direction, i.e. perpendicular to the light propagation direction (along the *x*-direction). We designed section length (L_{SWG}) and the

widths of the filling gaps (W_G) and lateral Si strips (W_B) to minimize the back-reflections. Figure 3a shows the grating reflectivity, calculated by 3-D FDTD, as a function of the gap width (W_G) and the length of an anti-reflection section (L_{SWG}). The transversal SWG period (Λ_{SWG}) was fixed to 400 nm, being small enough to suppress diffraction effects[14, 15]. According to these simulations, the reflectivity can be minimized for different SWG configuration, thereby this approach provide a good design flexibility. In Figure 3b, we compare the spectral performance of the reflectivity for the grating coupler designs with and without the SWG anti-reflection stage, considering L_{SWG} = 255 nm and W_G = 100 nm[39]. The proposed SWG transition stage yields an eight-fold reduction in grating reflectivity, from a 16% (-8 dB) to 2% (-17 dB) at a reference wavelength of 1.55 µm. It is worth mentioning that the proposed SWG metamaterial transition minimizes the back-reflections in the waveguide-to-grating junction across broad spectral range, exceeding 100 nm.
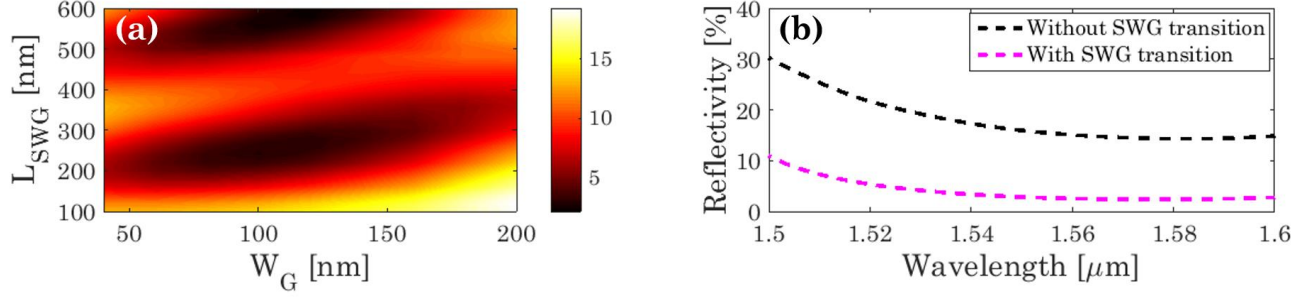

Figure 3. (a) 2-D contour map of the grating reflectivity as a function of the length of the SWG transition and the width of transversal gaps. (b) Spectral evolution of the reflectivity for nominal grating coupler designs, with and without the SWG transition stage, as predicted by 3-D FDTD calculations.

It is worth highlighting that the implementation of SWG reflection-cancelling stage does not affect the grating directionality. According to our 3-D FDTD simulations, the grating coupler with SWG-index engineered transition still provides a directionality higher that 98%, as shown in Figure 2e. We calculated the coupling efficiency for both grating coupler designs, with and without the SWG transition. As shown in Figures 4a and 4b, both 2-D and 3-D calculations predict a coupling loss of around -2 dB for both coupler designs, with an off-vertical fiber angle of 22°. Apodization techniques, as will be discussed in *Section 4*, may advantageously be utilized to improve the overall coupling performance, which in turn, allows us to deeply exploit the potential of the *L*-shaped surface grating couplers.
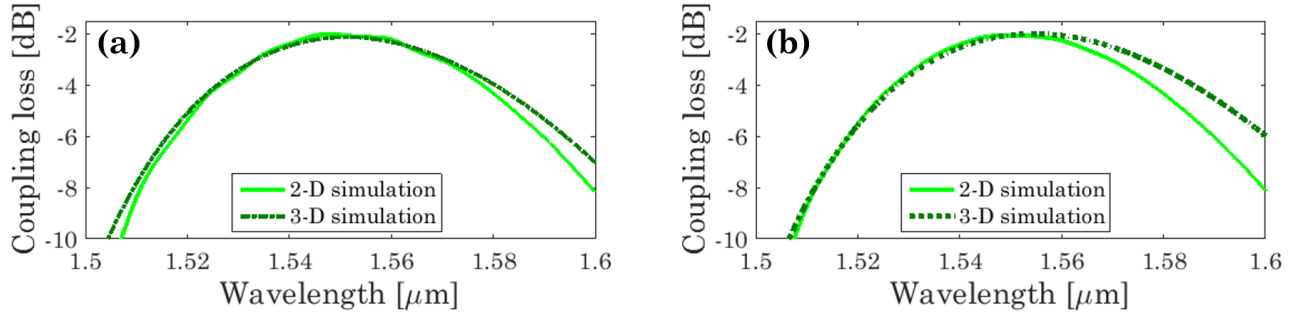

Figure 4. 2-D and 3-D calculations of the overall coupling losses as a function of a wavelength for nominal grating coupler designs (a) without and (b) with a SWG-index-engineered transition.

3. FABRICATION AND OPTICAL TESTING

Fiber-chip grating couplers were fabricated using a 300 mm SOI photonic platform with a 193-nm deep-UV optical lithography. The vertical dimensions are composed 300-nm-thick Si layer and 720-nm-thick buried oxide (BOX) layer. The double-level etching process was utilized to define the geometry of the grating coupler, with a 150 nm partial Si etch level for shallow-etch trenches and 300 nm deep etching for full-etch grating trenches and interconnecting strip waveguides, respectively. The grating couplers were 15-µm-wide and 21-µm-long, and were connected to the single-mode waveguides by adiabatic tapers with a length of 500 µm. Finally, fabricated devices were covered by a layer of silicon dioxide (SiO_2), which acts as a protection layer. The scanning electron microscopy (SEM) images of fabricated double-etch *L*-shaped surface grating couplers are shown in Figure 5d.
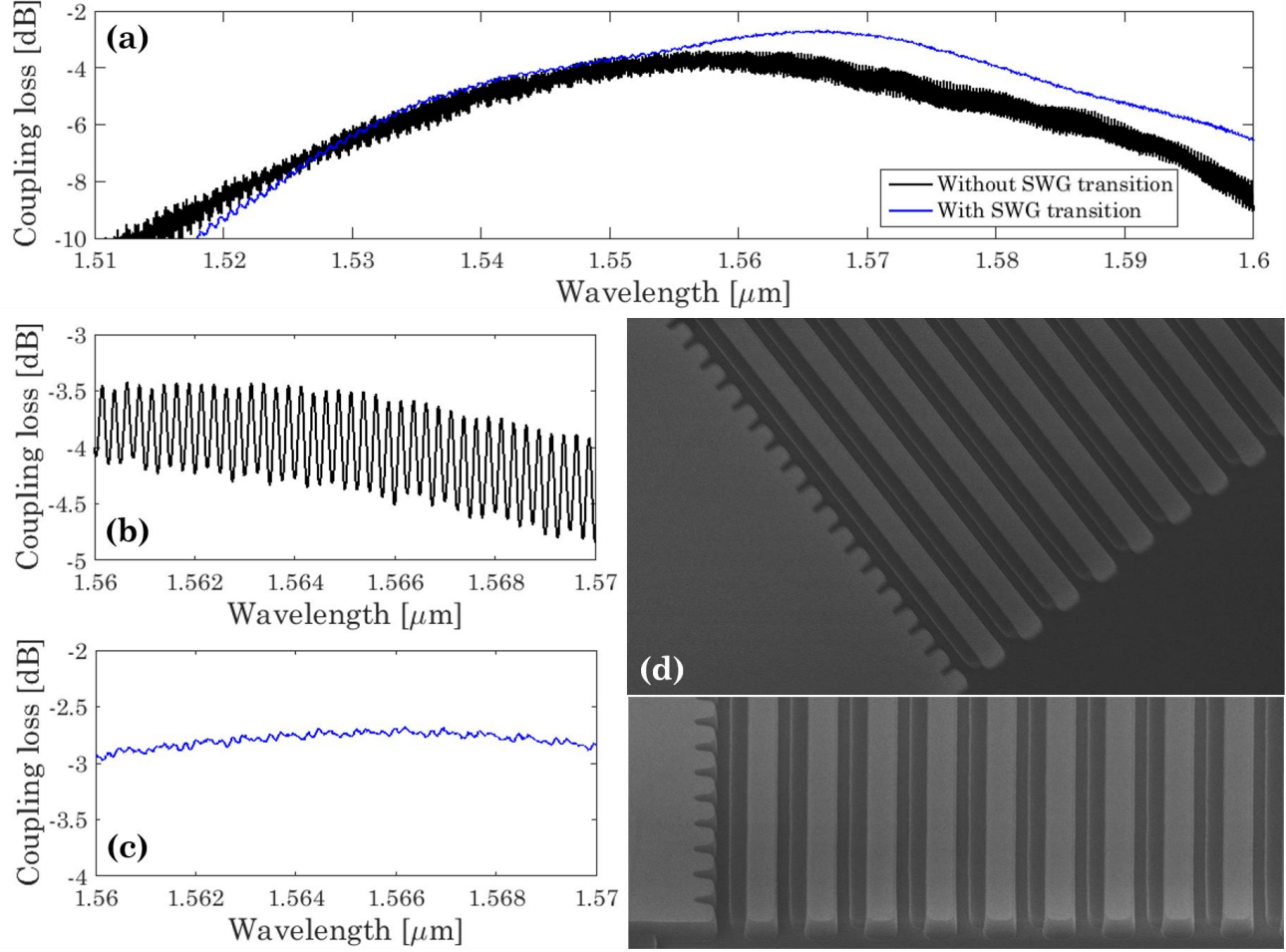
Figure 5. (a) Tested coupling loss as a function of a wavelength for both *L*-shaped grating designs. Detail look on a response of grating couplers: (b) without and (c) with SWG transition stage. (d) SEM images of fabricated *L*-shaped grating couplers.

Fabricated fiber-chip grating couplers were characterized in a back-to-back testing configuration. Cleaved single-mode optical fibers (SMF-28) were used as external access ports at the input and the output of the Si chip. The overall fiber-chip coupling efficiency was determined from the insertion loss measurements of two identical surface grating couplers with a back-to-back arrangement.

The measured fiber-chip coupling efficiencies, with and without a SWG transition stage, are shown in Figures 5a - 5c. More specifically, an experimental peak coupling efficiency of -3.4 dB near a wavelength of 1560 nm, with a 3-dB bandwidth of 46 nm, was tested for a grating coupler design without the SWG transition. Here, the spectral response of the grating coupler exhibits noticeable Fabry-Perrot fringes. From the amplitude of fringes, which varies between 0.7 dB and 0.85 dB and a periodicity of ~0.26 nm, we estimated a grating reflectivity of ~8% (-11 dB). The origin of these ripples is attributed to the back-reflections caused by the large discontinuity at the interface between the grating and the injection waveguide. Conversely, for a grating coupler with a SWG transition stage, the tested coupling efficiency reaches the peak of -2.7 dB at the wavelength of 1565 nm, with a coupling bandwidth of 62 nm. In this case, the coupler spectral response still shows some residual fringes, yet of comparatively smaller amplitudes up to 0.1 dB. This yields a reflectivity of ~1% (-20 dB), which is an eight-fold reduction in the measured back-reflections.

4. *L*-SHAPED GRATING COUPLERS OF SUB-DECIBEL LOSSES

In order to further improve the performance of the blazed surface grating couplers with a *L*-shaped geometry, the grating coupler is apodized by using SWG refractive index engineering. The apodization was performed by varying the effective refractive index of the SWG metamaterial in the etched grating trenches, both deep- and shallow-etch segments, along

the propagation direction (*z*-direction) to match the near-field profile of the radiated grating beam to the mode of SMF-28 optical fiber, i.e. to a Gaussian-like fiber mode profile of a 10.4 μm mode field diameter (MFD) at a central wavelength of 1.55 μm. By adjusting the SWG filling factor, defined as $W_{G,i}/\Lambda_{SWG}$, a wide range of SWG refractive indexes may be synthesized[14, 15], yet keeping critical dimensions compatible with the deep-UV optical lithography[5-8]. The optimal apodized device geometry was determined according to design strategy reported in Refs.[16-18].
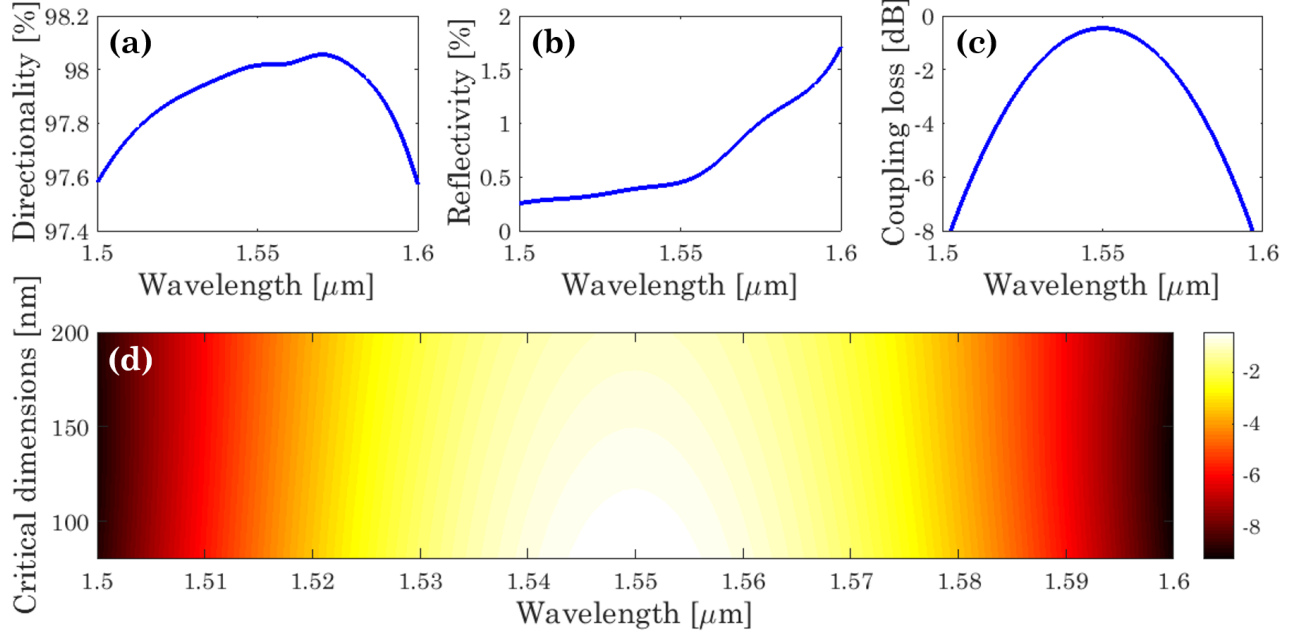

Figure 6. Estimated spectral performance of a *L*-shaped apodized fiber-chip grating coupler: (a) directionality; (b) reflectivity; and (c) coupling loss. (d) 2-D contour map of the coupling loss as a function of the wavelength and the minimum feature sizes.

According to our design predictions, the apodized *L*-shaped grating coupler yields a fiber-chip coupling of -0.45 dB, with a directionality of 98% and low back-reflections of 0.45% (-23.5 dB). The calculated 1-dB and 3-dB coupling bandwidth of the device is 34 nm and 59 nm, respectively. The spectral performance of a proposed *L*-shaped apodized grating coupler is shown in Figures 6a - 6c. Furthermore, the apodized *L*-shaped fiber-chip grating couplers also exhibits an improved robustness in respect to the different restrictions for minimum feature sizes. In particular, as shown in Figure 6d, the apodized *L*-shaped coupler designs predict an impressive coupling performance variability from -0.45 dB to -1 dB, for a critical dimensions variation in a range from 80 nm to 200 nm, thereby affording a fiber-chip coupling loss penalty of only 0.55 dB. These features of the proposed high-directionality grating coupler with a SWG metamaterial refractive index apodization hold the promise to realize integrated circuits that require efficient, robust, and foundry-compatible fiber-chip optical interfaces for deployment of silicon nanophotonic technology in large-volume applications.

5. CONCLUSION

In summary, we reported on the design, fabrication, and experimental demonstration of SWG-index-engineered fiber-chip grating couplers that simultaneously afford a high-directionality and a low-reflectivity, favoring a simplified *L*-shaped device geometry. The coupling devices were seamlessly realized on a 300 mm SOI wafer in a foundry-compatible fabrication flow, including 193 nm deep-UV optical lithography and double-level dry etching process. The fabricated grating couplers yielded a tested fiber-chip coupling efficiency up to -2.7 dB, with a 3-dB bandwidth of 62 nm. Furthermore, we also demonstrated by experiments that a short SWG transition stage effectively reduced the reflectivity down to 1%. This was an eight-fold enhancement in comparison to the conventional blazed grating couplers. In addition, we also theoretically elaborated a *L*-shaped fiber-chip grating coupler apodized by means of SWG metamaterial refractive index engineering that predicts a sub-decibel coupling efficiency of -0.45 dB. Coupling device predicts a large tolerance to the minimum feature size restrictions, being critical for device fabrication as well as for the

pattern fidelity of the SWG structures. These results prove the desired compatibility with the large-volume manufacturing processes, thereby opening a promising route towards further deployment of high-performance and price-reduced fiber-chip coupling interfaces in silicon nanophotonic applications.

ACKNOWLEDGEMENTS

REFERENCES

[1] Vivien, L. and Pavesi, L., [Handbook of Silicon Photonics], CRC Press, (2013).
[2] Rickman, A., "The commercialization of silicon photonics," Nature Photonics 8(8), 579-582 (2014).
[3] Hochberg, M. and Baehr-Jones, T., "Towards fabless silicon photonics," Nature Photonics 4(8), 492-494 (2010).
[4] Lim, A-J., Song, J., Fang, Q., Li, C., Tu, X., Duan, N., Chen, K. K., tern, R.-C., and Liow, T.-Y., "Review of silicon photonics foundry efforts," IEEE Journal of Selected Topics in Quantum Electronics 20(4), 405-416 (2014).
[5] Xu, D.-X., Schmid, J. H., Reed, G. T., Mashanovich, G. Z., Thomson, D. J., Nedeljkovic, M., Chen, X., Thourhout, D. V., Keyvaninia, S., and Selvaraja, S. K., "Silicon photonic integration platform: Have we found the sweet spot?," IEEE Selected Topics in Quantum Electronics 20(4), 189-205 (2014).
[6] Mekis, A., Gloeckner, S., Masini, G., Narasimha, A., Pinguet, T., Sahni, S., and De Dobbelaere, P., "A Grating-Coupler-Enabled CMOS Photonic Platform," IEEE Selected Topics in Quantum Electronics 17(3), 597-608 (2011).
[7] Kopp, Ch., Bernabe, S., Bakir, B. B., Fédéli, J.-M., Orobtchouk, R., Schrank, F., Porte, H., Zimmermann, L., and Tekin, T., "Silicon photonic circuits: On-CMOS integration, fiber optical coupling, and packaging," IEEE Selected Topics in Quantum Electronics 17(3), 498-509 (2011).
[8] Boeuf, F., Cremer, S., Temporiti, E., Fere, M., Shaw, M., Baudot, Ch., Vulliet, N., Pinguet, T., Mekis, A., Masini, G., Petiton, H., Le Maitre, P., Traldi, M., and Maggi, L., "Silicon Photonics R&D and Manufacturing on 300-mm Wafer Platform," IEEE Journal of Lightwave Technology 34(2), 286-295 (2016).
[9] Cheben, P., Schmid, J. H., Wang, S., Xu, D.-X., Vachon, M., Janz, S., Lapointe, J., Painchaud, Y., and Picard, M.-J., "Broadband polarization independent nanophotonic coupler for silicon waveguides with ultra-high efficiency," Optics Express 23(17), 22553-22563 (2015).
[10] Barwicz, T., Janta-Polczynski, A., Khater, M., Thibodeau, Y., Laidy, R., Maling, J., Martel, S., Engelmann, S., Orcutt, J. S., Fortier, P., and Green, W. M. J., "An O-band metamaterial converter interfacing standard optical fibers to silicon nanophotonic waveguides," Proc. Optical Fiber Communication Conference (OFC), paper Th3F.3 (2015).
[11] Li, C., Zhang, H., Yu, M., and Lo, G. Q., "CMOS-compatible high efficiency double-etch apodized waveguide grating coupler," Optics Express 21(7), 7868-7874 (2013).
[12] Taillaert, D., Bienstman, P., and Baest, R., "Compact efficient broadband grating coupler for silicon-on-insulator waveguides," Optics Letters 29(23), 2749-2751 (2004).
[13] Chen, X., Li, Ch., Fung, Ch. K. Y., Lo, M. G., and Tsang, H. K., "Apodized Waveguide Grating Couplers for Efficient Coupling to Optical Fibers," IEEE Photonics Technology Letters 22(15), 1156-1158 (2010).
[14] Halir, R., Cheben, P., Janz, S., Xu, D.-X., Molina-Fernandez, I., and Wangüemert-Perez, J. G., "Waveguide grating coupler with subwavelength microstructures," Optics Letters 34(9), 1408-1410 (2009).
[15] Halir, R., Cheben, P., Schmid, J. H., Ma, R, Bedard, D., Janz, S., Xu, D.-X., Densmore, A., Lapointe, J., Molina-Fernandez, I., "Continuously apodized fiber-to-chip surface grating coupler with refractive index engineered sub-wavelength structure," Optics Letters 35(19), 3243-3245 (2010).
[16] Benedikovic, D., Cheben, P., Schmid, J. H., Xu, D.-X., Lapointe, J., Wang, S., Halir, R., Ortega-Moñux, Janz, S., and Dado, M., "High-efficiency single etch step apodized surface grating coupler using subwavelength structure," Laser and Photonics Reviews 8(6), 93-97 (2014).
[17] Benedikovic, D., Cheben, P., Schmid, J. H., Xu, D.-X., Lamontagne, B., Wang, S., Lapointe, J., Halir, R., Ortega-Moñux, A., Janz, S., Dado, M., "Subwavelength index engineered surface grating coupler with sub-decibel efficiency for 220-nm silicon-on-insulator waveguides," Optics Express 23(17), 22628-22635 (2015).

[18] Benedikovic, D., Alonso-Ramos, C., Cheben, P., Schmid, J. H. Wang, S., Halir, R., Ortega-Moñux, A., Xu, D.-X., Vivien, L., Lapointe, J., Janz, S., and Dado, M., "Single-etch subwavelength engineered fiber-chip grating couplers for 1.3 μm datacom wavelength band," Optics Express 24(12), 12893-12904 (2016).

[19] Roelkens, G., Van Thourhout, D., and Baets, R., "High efficiency Silicon-on-Insulator grating coupler based on a poly-Silicon overlayer," Optics Express 14(24), 11622-11630 (2006).

[20] Vermeulen, D., Selvaraja, S., Verheyen, P., Lepage, G., Boagerts, W., Absil, P., Van Thourhout, D., and Roelkens, G., "High-efficiency fiber-to-chip grating couplers realized using an advanced CMOS-compatible Silicon-On-Insulator platform," Optics Express 18(17), 18278-18283 (2010).

[21] Chen, H.-Y. and Yang, K.-Ch., "Design of a high-efficiency grating coupler based on a silicon nitride overlayer for silicon-on-insulator waveguides," Applied Optics 49(33), 6455-6462 (2010).

[22] Yang, S., Zhang, Y., Baehr-Jones, T., and Hochberg, M., "High efficiency germanium-assisted grating coupler," Optics Express 22(25), 30607-30612 (2014).

[23] Zaoui, W. S., Kunze, A., Vogel, W., Berroth, M., Butschke J., Letzkus, F., and Burghartz, J., "Bringing the gap between optical fibers and silicon photonic integrated circuits," Optics Express 22(2), 1277-1286 (2014).

[24] Ding, Y., Peucheret, Ch., Ou, H., and Yvind, K., "Fully etched apodized grating coupler on the SOI platform with -0.58 dB coupling efficiency," Optics Letters 39(18), 5348-5350 (2014).

[25] Van Laere, F., Roelkens, G., Ayre, M., Schrauwen, J., Taillert, D., Van Thourhout, D., Krauss, T. F., and Baets, R., "Compact and highly efficient grating couplers between optical fiber and nanophotonic waveguides," IEEE Journal of Lightwave Technology 25(1), 151-156 (2007).

[26] Wang, Z., Tsang, Y., Wosinki, L., and He, S., "Experimental demonstration of high-efficiency polarization splitter based on a one-dimensional grating with a Bragg reflector underneath," IEEE Photonics Technology Letters 22(21), 1568-1570 (2010).

[27] Baudot, C., Dutartre, D., Souhaité, A., Vulliet, N., Jones, A., Ries, M., Mekis, A., Verslegers, L., Sun, P., Chi, Y., Cremer, S., Gourhant, O., Benoit, D., Courgoulet, G., Perrot, C., Broussous, L., Pinguet, T., Siniviant, J., and Boeuf, F., "Low Cost 300 mm double-SOI substrate for low insertion loss 1D & 2D grating couplers," Proc. of IEEE 11-th International Conference on Group IV Photonics, 137–138 (2014).

[28] Sacher, W. D., Huang, Y., Ding, L., Taylor, B. J. F., Jayatilleka, H., Lo, G.-Q., and Poon, J. K. S., "Wide bandwidth and high coupling efficiency Si_3N_4-on-SOI dual-level grating coupler," Optics Express 22(9), 10938-10947 (2014).

[29] Wade, M. T., Pavanello, F., Kumar, R., Gentry, C. M., Atabaki, A., Ram, R., Stojanovic, V., and Popovic, M., "75% Efficient Wide Bandwidth Grating Couplers in a 45 nm Microelectronics CMOS Process," Proc. of IEEE Optical Interconnects Conference, 46-47 (2015).

[30] Notaros, J., Pavanello, F., Wade, M. T., Gentry, C., Atabaki, A., Alloatti, L., Ram, R. J., and Popovic, M., "Ultra Efficient CMOS Fiber-to-Chip Grating Couplers," Proc. Optical Fiber Communication Conference (OFC), paper M2I.5 (2016).

[31] Can, Z., Jing-Hua, S., Xi, X., Wei-Min, S., Xiao-Jun, Z., Tao, C., Jin-Zhong, Y., and Yu-De, Y., "High efficiency grating coupler for coupling between single-mode fiber and SOI waveguides," Chinese Physics Letters 30(1), 014207 (2013).

[32] Alonso-Ramos, C., Ortega-Moñux, A., Molina-Fernandez, I., Cheben, P., Zavargo-Peche, L., and Halir, R., "Efficient fiber-to-chip grating coupler for micrometric SOI rib waveguides," Optics Express 18(14), 15189-15200 (2010).

[33] Alonso-Ramos, C., Cheben, P., Ortega-Moñux, A., Schmid, J. H., Xu, D.-X., and Molina-Fernández, I., "Fiber-chip grating coupler based on interleaved trenches with directionality exceeding 95%," Optics Letters 39(18), 5351–5354 (2014).

[34] Benedikovic, D., Alonso-Ramos, C., Cheben, P., Schmid, J. H., Wang, S., Xu, D.-X., Lapointe, J., Janz, S., Halir, R., Ortega-Moñux, A., Wangüemert-Pérez, J. G., Molina-Fernández, I., Fédéli, J.-M., Vivien, L., and Dado, M., "High-directionality fiber-chip grating coupler with interleaved trenches and subwavelength index-matching structure," Optics Letters 40(18), 4190–4193 (2015).

[35] Watanabe, T., Ayata, M., Koch, U., Fedoryshyn, Y., and Leuthold, J., "Perpendicular Grating Coupler Based on a Blazed Antiback-Reflection Structure," IEEE Journal of Lightwave Technology 35(21), 4663-4669 (2017).

[36] Chen, X., Thomson, D. J., Crudginton, L., Khokhar, A. Z., and Reed, T. G., "Dual-etch apodised grating couplers for efficient fibre-chip coupling near 1310 nm wavelength," Optics Express 25(15), 17864-17871 (2017).

[37] Chen, Y., Halir, R., Molina-Fernández, I., Cheben, P., and He, J.-J., "High-efficiency apodized-imaging chip-fiber grating coupler for silicon nitride waveguides," Optics Letters 41(21), 5059-5062 (2016).

[38] Chen, Y., Dominguez-Bucio, T., Khokhar, A. Z., Banakar, M., Grabska, K., Gardes, F. Y., Halir, R., Molina-Fernández, I., Cheben, P., and He, J.-J., "Experimental demonstration of an apodized-imaging chip-fiber grating coupler for Si$_3$N$_4$ waveguides," Optics Letters 42(18), 3566-3569 (2017).

[39] Benedikovic, D., Alonso-Ramos, C., Perez-Galacho, D., Guerber, S., Vakarin, V., Marcaud, G., Le Roux, X., Cassan, E., Marris-Morini, D., Cheben, P., Boeuf, F., Baudot, Ch., and Vivien, L., "L-shaped fiber-chip grating couplers with high directionality and low reflectivity fabricated with deep-UV lithography" Optics Letters 42(17), 3439-3442 (2017).

[40] Marris-Morini, D., Virot, L., Baudot, Ch., Fédéli, J.-M., Rasigade, G., Perez-Galacho, D., Hartmann, J.-M., Oliver, S., Brindel, P., Crozat, P., Boeuf, F., and Vivien, L., "A 40 Gbit/s optical link on a 300-mm silicon platform," Optics Express 22(6), 6674-6679 (2014).

[41] Zavargo-Peche, L., Ortega- Moñux, A., Wangüemert-Pérez, J. G., and Molina-Fernandez, I., "Fourier based combined techniques to design novel sub-wavelength optical integrated devices," Progress in Electromagnetic Research 123, 447-465 (2012).

[42] Lumerical Solutions, Inc. [Online]. Available: http://www.lumerical.com.

[43] Cheben, P., Xu, D.-X., Janz, S., and Densmore, A., "Subwavelength waveguide grating for mode conversion and light coupling in integrated optics," Optics Express 14(11), 4695-4702 (2006).

[44] Bock, P. J., Cheben, P., Schmid, J. H., Lapointe, J., Delage, A., Janz, S., Aers, G. C., Xu, D.-X., Densmore, A., and Hall, T. J., "Subwavelength grating periodic structures in silicon-on-insulator: a new type of microphotonic waveguide," Optics Express 18(19), 20251-20262 (2010).

[45] Cheben, P., Bock, P. J., Schmid, J. H., Lapointe, J., Janz, S., Xu, D.-X., Densmore, A., Delage, A., Lamontagne, B., and Hall, T. J., "Refractive index engineering with subwavelength gratings for efficient microphotonic couplers and planar waveguide multiplexers," Optics Letters 35(15), 2526-2528 (2010).

[46] Halir, R., Bock, P., Cheben, P., Ortega-Moñux, A., Alonso-Ramos, C., Schmid, J. H., Lapointe, J., Xu, D.-X., Wangüemert-Pérez, J. G., Molina-Fernández, I., and Janz, S., "Waveguide sub-wavelength structures: a review of principles and applications," Laser & Photonics Reviews 9(1), 25-49 (2015).

[47] Halir, R., Cheben, P., Luque-González, J. M., Sarmiento-Merenguel, J. D., Schmid, J. H., Wangüemert-Pérez, G., Xu, D.-X., Wang, S., Ortega-Moñux, A., and Molina-Fernández, I., "Ultra-broadband nanophotonic beam splitter using an anisotropic sub-wavelength metamaterial," Laser & Photonics Reviews 10(6), 1039–1046 (2016).

[48] Yun, H., Wang, Y., Zhang, F., Lu, Z., Lin, S., Chrostowski, L., and Jaeger, N. A. F., "Broadband 2 × 2 adiabatic 3 dB coupler using silicon-on-insulator sub-wavelength grating waveguides," Optics Letters 41(13), 3041–3044 (2016).

[49] Wang, Y., Shi, W., Wang, X., Lu, Z., Caverley, M., Bojko, R., Chrostowski, L., and Jaeger, N. A. F., "Design of broadband subwavelength grating couplers with low back reflection," Optics Letters 40(20), 4647–4650 (2015).

[50] Wang, J., Glesk, I., and Chen, L. R., "Subwavelength grating filtering devices," Optics Express 22(13), 15335–15345 (2014).

[51] Pérez-Galacho, D., Alonso-Ramos, C., Mazeas, F., Le Roux, X., Oser, D., Zhang, W., Marris-Morini, D., Labonté, L., Tanzilli, S., Cassan, E., and Vivien, L., "Optical pump-rejection filter based on silicon sub-wavelength engineered photonic structures," Optics Letters 42(8), 1468–1471 (2017).

[52] Ctyroky, J., Wangüemert-Pérez, J. G., Kwiecien, P., Richter, I., Litvik, J., Schmid, J. H., Molina-Fernández, I., Ortega-Moñux, A., Dado, M., and Cheben, P., "Design of narrowband spectral filters in subwavelength grating metamaterial waveguides," Optics Express 26(1), 179-194 (2018).

[53] Wangüemert-Pérez, J. G., Cheben, P., Ortega-Moñux, A., Alonso-Ramos, C., Pérez-Galacho, D., Halir, R., Molina-Fernández, I., Xu, D.-X., and Schmid, J. H., "Evanescent field waveguide sensing with subwavelength grating structures in silicon-on-insulator," Optics Letters 39(15), 4442–4445 (2014).

[54] Flueckiger, J., Schmidt, S., Donzella, V., Sherwali, A., Ratner, D. M., Chrostowski, L., and Cheung, K. C., "Sub-wavelength grating for enhanced ring resonator biosensor," Optics Express 24(14), 15672–15686 (2016).

[55] Huang, L., Yan, H., Xu, X., Chakravarty, S., Tang, N., Tian, H., Chen, R. T., "Improving the detection limit for on-chip photonic sensors based on subwavelength grating racetrack resonators," Optics Express 25(9), 10527-10535 (2017).

[56] Penades, J. S., Ortega-Moñux, A., Nedeljkovic, M., Wangüemert-Pérez, J. G., Halir, R., Khokhar, A. Z., Alonso-Ramos, C., Qu, Z., Molina-Fernández, I., Cheben, P., and Mashanovich, G. Z., "Suspended silicon mid-infrared waveguide devices with subwavelength grating metamaterial cladding," Optics Express 24(20), 22908–22916 (2016).

[57] Kang, J., Cheng, Z., Zhou, W., Xiao, T.-H., Gopalakrisna, K.-L., Takenaka, M., Tsang, H. K., and Goda, K., "Focusing subwavelength grating coupler for mid-infrared suspended membrane germanium waveguides," Optics Letters 42(11), 2094-2097 (2017).